arXiv:1404.2382v2 [gr-qc] 23 Jul 2014

Parameter estimation on compact binary coalescences with abruptly terminating gravitational waveforms

Ilya Mandel[1,2] ‡, Christopher P L Berry[1], Frank Ohme[3], Stephen Fairhurst[3], Will M Farr[1]

[1] School of Physics and Astronomy, University of Birmingham, Edgbaston, Birmingham B15 2TT, United Kingdom

[2] National Institute for Theoretical Physics (NITheP), Western Cape, South Africa

[3] School of Physics and Astronomy, Cardiff University, Cardiff, CF24 3AA, United Kingdom

Abstract. Gravitational-wave astronomy seeks to extract information about astrophysical systems from the gravitational-wave signals they emit. For coalescing compact-binary sources this requires accurate model templates for the inspiral and, potentially, the subsequent merger and ringdown. Models with frequency-domain waveforms that terminate abruptly in the sensitive band of the detector are often used for parameter-estimation studies. We show that the abrupt waveform termination contains significant information that affects parameter-estimation accuracy. If the sharp cutoff is not physically motivated, this extra information can lead to misleadingly good accuracy claims. We also show that using waveforms with a cutoff as templates to recover complete signals can lead to biases in parameter estimates. We evaluate when the information content in the cutoff is likely to be important in both cases. We also point out that the standard Fisher matrix formalism, frequently employed for approximately predicting parameter-estimation accuracy, cannot properly incorporate an abrupt cutoff that is present in both signals and templates; this observation explains some previously unexpected results found in the literature. These effects emphasize the importance of using complete waveforms with accurate merger and ringdown phases for parameter estimation.

PACS numbers: 02.50.Tt, 04.30.–w, 95.85.Sz

‡ email:imandel@star.sr.bham.ac.uk

1. Introduction

Gravitational-wave (GW) astronomy endeavours to infer the properties of astrophysical systems from the gravitational radiation they emit. For ground-based detectors, such as the Laser Interferometer Gravitational-wave Observatory (LIGO) and Virgo [1, 2], a principal GW source are binaries consisting of neutron stars or stellar-mass black holes that inspiral and eventually coalesce as GWs carry away energy and angular momentum. Parameters of interest for these systems include the component masses and spins and the location and orientation of the binary. With the upcoming advanced generation of GW detectors [3, 4], which are expected to make the first detections of coalescing black-hole and neutron-star binaries [5, 6], efforts to predict parameter-estimation accuracy have intensified.

Over the past two decades, a variety of techniques have been used for predicting the accuracy with which parameters can be extracted from a detected GW signal. The Fisher information matrix (FIM) formalism has been particularly popular because of its low computational cost and ease of use [7]. Dozens of studies have used the FIM tool, including the classic work of [8, 9, 10], ranging in applications from tests of GR [11, 12] to sky-localization predictions for multi-messenger astronomy [13, 14, 15]. More recently, alternatives to the FIM formalism have been considered, e.g., [16, 17, 18]. Finally, as computational resources have expanded, more costly Bayesian techniques [19] have been employed to compute the full posterior probability density functions of the signal parameters. These techniques, based on stochastically sampling the parameter space with methods such as Markov chain Monte Carlo and nested sampling, have been used to consider measurements of masses and spins for different classes of systems and the sky-localization ability of different network configurations, e.g., [20, 21, 22, 23, 24].

Despite the differences in methodology, all of the studies referenced above, and many others, share one common feature: they use waveforms that terminate abruptly in the band of the detectors. We do not expect most real GW signals to exhibit such a steep falloff, but instead that they evolve smoothly through inspiral, merger and ringdown phases. However, accurate waveforms that included all phases of the GW signal were not available until recent advances in numerical relativity (see [25, 26] for recent reviews) allowed analytical waveform families to be constructed by calibrating against numerical results, e.g., [27, 28, 29, 30, 31, 32, 33]. Meanwhile, inspiral-only waveforms based on the post-Newtonian expansion and terminating at the innermost stable circular orbit (ISCO) have been known for many years [34] and are computationally inexpensive to calculate. Consequently, it was natural for the early studies to make use of these waveforms. Even now, there are cases where it is beneficial to use post-Newtonian waveforms with an abrupt termination.

Frequency-domain waveforms based on the stationary-phase approximation [35, 36, 37] are particularly well suited to both analytical and numerical studies. Such a waveform, terminated at the ISCO, can be written as

$$\tilde{h}(f) = A(f) \exp\left[i\Psi(f)\right] H(f_{\rm ISCO} - f) \tag{1}$$

$$\equiv \tilde{h}^0(f)H(f_{\rm ISCO} - f), \tag{2}$$

where $f_{\rm ISCO}$ is the GW frequency at the ISCO, and H is the Heaviside step function. These have been generally used for both FIM calculations and parameter-estimation studies (as discussed above), with a few notable exceptions including [38, 39, 40], as well as for gravitational-wave searches [41, 42, 43]. However, the impact of the step function, i.e., the sharp waveform cutoff, is typically ignored in these applications.

In this paper, we investigate in detail the effect of using waveforms with a sharp cutoff in the frequency domain on parameter recovery. After briefly recalling the likelihood and FIM formalism (Sec. 2), we begin by considering the case where both the true signal and the waveforms used to recover it terminate abruptly. We show that the abrupt termination significantly alters the information content of the signal. In particular, while the accuracy of measurement typically scales inversely with the signal-to-noise ratio (SNR), parameters associated with an abrupt cutoff can be measured with an uncertainty proportional to the square of the inverse SNR (Sec. 3.1). We describe the regime in which the abrupt waveform termination significantly impacts parameter-estimation accuracy (Sec. 3.2) and derive the likelihood function for a data set given a model with a sharp waveform cutoff (Sec. 3.3). Subsequently, we consider the impact of the abrupt waveform termination on the FIM formalism, and explain the apparent violation of the Cramér–Rao bound found by [44], whose Bayesian confidence intervals on mass parameters were a few times smaller than those predicted by their FIM (Sec. 3.4).

Then, in Sec. 4, we investigate the impact of using template waveforms with an abrupt cutoff in searching for, and estimating the parameters of, signals which extend smoothly through merger and ringdown. We show that, at leading order, the parameter accuracies given by the FIM are correct if inspiral-only information is used, although the presence of a merger and ringdown can lead to a systematic offset in the recovered parameters and the use of full inspiral–merger–ringdown waveforms for the analysis could allow for more accurate parameter estimation. We evaluate this bias in recovered parameters and identify the regime where cutoff waveforms introduce significant bias into signal recovery.

While we limit our discussion to the specific application to GW signals, we hope it is of interest to other fields which employ similar parameter-estimation techniques.

2. Likelihood and Fisher information matrix

In GW astronomy, the observed data d is generally modeled as a sum of a waveform h, which is a function of system parameters $\vec{\theta}_0$ according to an assumed waveform model, and an additive stationary and Gaussian noise n:

$$d(t) = h(\vec{\theta}_0; t) + n(t), \tag{3}$$

with the frequency-domain expectation value of n being

$$\mathrm{E}[\tilde{n}(f')\tilde{n}^*(f)] = \delta(f - f')S_n(f), \tag{4}$$

where $\tilde{x}(f)$ is the Fourier transform of $x(t)$, $\tilde{x}^*(f)$ is the complex conjugate of $\tilde{x}(f)$, and $S_n(f)$ is the frequency-dependent noise power spectral density.

Both the detection of a GW signal and the extraction of astrophysical source parameters rely on calculating the likelihood L of observing a data set d given a waveform model $h(\vec{\theta})$. The logarithm of this likelihood, ignoring an additive constant, is given by

$$\log L(\vec{\theta}) \equiv \log p(d|\vec{\theta}) = -\frac{1}{2}\Big\langle d - h(\vec{\theta})\Big| d - h(\vec{\theta})\Big\rangle, \tag{5}$$

where the inner product is defined as

$$\langle a|b\rangle = 4\ \mathrm{Re}\int_0^\infty \frac{\tilde{a}(f)\tilde{b}^*(f)}{S_n(f)}\,\mathrm{d}f. \tag{6}$$

The expectation value of the likelihood over noise realizations $\mathrm{E}[\log L(\vec{\theta})]$ can be expanded around its value at the signal parameters in a Taylor series *if* the likelihood is a smooth, differentiable function at the signal parameters; as we will show below, this condition fails for abruptly terminated templates. The lowest non-vanishing contribution to this Taylor expansion comes at the quadratic order in parameter deviations $\Delta\vec{\theta} \equiv \vec{\theta} - \vec{\theta}_0$, and is proportional to the FIM Γ_{ij} which is defined as

$$\Gamma_{ij}(\vec{\theta}_0) = \mathrm{E}\left[-\frac{\partial}{\partial\theta_i}\frac{\partial}{\partial\theta_j}\log L(\vec{\theta})\right]. \tag{7}$$

Here, the expectation value is taken over the possible measurements given true parameters $\vec{\theta}_0$, i.e., over possible noise realizations n. In the GW data-analysis context, the FIM is given by

$$\begin{aligned}\Gamma_{ij}(\vec{\theta}_0) &= \mathrm{E}[-\langle d|h_{,ij}\rangle + \langle h_{,i}|h_{,j}\rangle + \langle h|h_{,ij}\rangle] \\ &= \langle h_{,i}|h_{,j}\rangle,\end{aligned} \tag{8}$$

where $h_{,i} \equiv \partial h/\partial\theta_i$, and we have used the fact that the expectation value of the noise vanishes.

In the high-SNR limit, parameters are constrained sufficiently well that only small variations compared to their true values are probable, hence the linear-signal approximation should hold, $h(\vec{\theta}) \approx h(\vec{\theta}_0) + \sum_i h_{,i}\Delta\theta_i$. In the linear-signal, high-SNR approximation, the covariance matrix Σ_{ij} can be approximated as the inverse FIM [7]:

$$\Sigma_{ij} \simeq \left(\Gamma^{-1}\right)_{ij} = \langle h_{,i}|h_{,j}\rangle^{-1}. \tag{9}$$

What constitutes high SNR depends upon the signal, hence this approximation must be checked for each source type (cf. [45]).

Regardless of the validity of this approximation, the FIM always yields the Cramér–Rao lower bound (see, e.g., [7]) on the expectation over noise realizations of the variance of any unbiased estimator for $\vec{\theta}_0$ at fixed $\vec{\theta}_0$:

$$|\Sigma_{ij}| \geq \left|\left(\Gamma^{-1}\right)_{ij}\right|. \tag{10}$$

Comparisons of FIM results against Monte Carlo studies [46] and Bayesian parameter estimation methods [44] have shown that the priors used in Bayesian analysis provide

additional information that, if not included in FIM analysis, can lead to apparent violations of the Cramér–Rao bound.

With the introduction of a sharp cutoff in the waveform, the picture changes dramatically. Rodriguez *et al.* [44] found that even when priors are accounted for, Bayesian analysis recovers confidence intervals on mass parameters that are a few times smaller than those predicted by the FIM, in apparent violation of the Cramér–Rao bound. However, for binary merger waveforms, the ISCO frequency depends on the parameters of the waveform, in particular the total mass. Thus, one should take into account the changing cutoff frequency when calculating the FIM. This is generally not done, and holds the key to understanding the apparent violation of the Cramér–Rao bound: there is extra information present in the sharp waveform cutoff, which is available to Bayesian techniques but not incorporated in these FIM calculations. We show how to add this information to the FIM in Sec. 3.4.

3. Effect of a sharp frequency cutoff

3.1. Accuracy of measuring a sharp cutoff

Although the accuracy of parameter estimation typically scales inversely with the SNR in the high-SNR limit, this does not happen when the waveform ends abruptly in-band. To demonstrate this, we first consider a toy scenario. We assume a waveform family of the form given in (1), where all parameters are fixed except for the cutoff frequency. This simplifies the inner product of (5) tremendously, because the only nonvanishing contribution comes from the frequency interval in which one waveform has terminated already but the other one has not (cf. [17]).

Let the cutoff frequency of the measured signal be f_0 and the template be terminated at $f_{\rm cut}$. We refrain from using the symbol $f_{\rm ISCO}$ for now, as we first neglect correlations with other physical parameters and view $f_{\rm cut}$ as the only free parameter. Let us further assume that the noise realization happens to be exactly zero for the particular measurement we undertook; this is done only to simplify calculations, as measurement accuracy is not affected by the choice of noise realization in the high-SNR limit. Equivalently, the same results could be obtained by averaging over an ensemble of noise realisations. The first-order expansion of the parameter-dependent part of (5) then reads

$$\begin{aligned} -2\log L(\vec{\theta}) = \langle \Delta h|\Delta h\rangle &= 4\left|\int_{f_0}^{f_{\rm cut}} \zeta(f)\,{\rm d}f\right| \\ &\approx 4\zeta(f_0)\,|f_0 - f_{\rm cut}|\,, \end{aligned} \tag{11}$$

where $\Delta h \equiv h(\vec{\theta}_0) - h(\vec{\theta})$ is the waveform difference, in this example $\Delta h = h^0(f)H(f_0 - f) - h^0(f)H(f_{\rm cut} - f)$, and the noise weighted signal power $\zeta(f)$ defined as

$$\zeta(f) = \frac{|A(f)|^2}{S_n(f)}. \tag{12}$$

The log likelihood scales *linearly* with the *absolute value* of $f_0 - f_{\rm cut}$; this is different from the usual quadratic scaling of the log likelihood with parameter variations, which permits a Taylor expansion and leads to the FIM derivation.

As ζ depends quadratically on the overall signal amplitude, we can write

$$4\zeta(f_0) \equiv \kappa(f_0)\rho^2, \tag{13}$$

where $\rho = \sqrt{\langle h|h\rangle}$ is the SNR and κ is some (f_0 dependent) constant.§

With these simplifications, we can infer the posterior probability of $f_{\rm cut}$ being the correct parameter, assuming a uniform prior on $f_{\rm cut} \in [0, \infty]$. The resulting probability density reads

$$p(f_{\rm cut}|d) = \frac{1}{Z}\exp\left(-\frac{\kappa\rho^2|f_{\rm cut} - f_0|}{2}\right), \tag{14}$$

where the normalization is given by

$$Z = \frac{2}{\kappa\rho^2}\left[2 - \exp\left(-\frac{\kappa\rho^2 f_0}{2}\right)\right]. \tag{15}$$

Calculating the expectation values over this distribution yields

$$\mathrm{E}[f_{\rm cut}] = f_0 + \mathcal{O}\left(\exp\left(-\frac{\kappa\rho^2 f_0}{2}\right)\right) \tag{16}$$

and

$$\mathrm{E}\left[f_{\rm cut}^2\right] = f_0^2 + \frac{8}{\kappa^2\rho^4} + \mathcal{O}\left(\exp\left(-\frac{\kappa\rho^2 f_0}{2}\right)\right). \tag{17}$$

The variance is

$$\begin{aligned}\sigma^2_{f_{\rm cut}} &= \mathrm{E}\left[f_{\rm cut}^2\right] - \left(\mathrm{E}[f_{\rm cut}]\right)^2 \\ &= \frac{8}{\kappa^2\rho^4} + \mathcal{O}\left(\exp\left(-\frac{\kappa\rho^2 f_0}{2}\right)\right);\end{aligned} \tag{18}$$

thus, we find that the uncertainty in the measurement of $f_{\rm cut}$ actually scales inversely with the square of the SNR.

This scaling of the measurement uncertainty with the inverse of the square of SNR, rather than the inverse of the SNR is, in fact, typical for problems with a sharp cutoff. For example, consider the problem of finding the minimum or maximum of some distribution (say, neutron-star spins) given N observations. Although generally the uncertainty in distribution parameters (e.g., the distribution mean) scales as $1/\sqrt{N}$, the accuracy with which a sharp cutoff can be measured scales as $1/N$ (cf. [47]).

3.2. Significance of an abrupt cutoff

In real GW searches, the cutoff frequency is often conveniently taken to be the frequency of the innermost stable circular orbit of a test particle orbiting a non-spinning black hole,

$$f_{\rm cut} \equiv f_{\rm ISCO} = \frac{1}{6^{3/2}\pi M}, \tag{19}$$

§ As an example, consider the (unrealistically) simple scenario where $\zeta(f)$ is constant for $0 \le f \le f_0$; in this case $\rho^2 = 4\zeta f_0$, hence $\kappa = 1/f_0$.

where $M = m_1 + m_2$ is identified as the total mass of the system. For black-hole binaries with two $10M_\odot$ components, $f_{\rm ISCO} = 220$ Hz is in the band of initial and advanced detectors; for binary neutron-star systems, the ISCO frequency of ~ 1500 Hz is sufficiently high that to be effectively out of band.

The accuracy of measuring $f_{\rm ISCO}$ depends on where this frequency falls on the detector's noise spectrum. However, it is usually not included in the set of independent parameters; rather, $f_{\rm ISCO}$ is defined by the correlation with mass-dependent parameters. We can nevertheless use the derivation of the previous section to gauge where such a parameter-dependent cutoff frequency is relevant.

In the previous section, we calculated the measurement uncertainty of $f_{\rm ISCO}$, given by (18), under the assumption that all other parameters are perfectly known. We denote this uncertainty $\sigma^{\rm abrupt}_{f_{\rm ISCO}}$ to highlight the inclusion of the cutoff, and re-express it as

$$\sigma^{\rm abrupt}_{f_{\rm ISCO}} \simeq \frac{1}{\sqrt{2}\zeta(f_{\rm ISCO})}. \tag{20}$$

Assuming perfect knowledge of the other parameters causes this to be an underestimation of the true uncertainty in determining the ISCO frequency.

Alternatively, we can compute the predicted parameter-estimation accuracy without taking the abrupt cutoff into account by using the naive, inspiral-only FIM Γ_{ij} that ignores the presence of the cutoff (see Sec. 3.4) and convert this to an estimate of the accuracy with which $f_{\rm ISCO}$ could be measured using the other parameters. We denote this $\sigma^{\rm naive}_{f_{\rm ISCO}}$. If the total mass M and the mass ratio $q = m_2/m_1$ are used to parametrize the binary with non-spinning components, the only non-vanishing partial derivative of $f_{\rm ISCO}$ with respect to the parameters is

$$\frac{\partial f_{\rm ISCO}}{\partial M} = -\frac{f_{\rm ISCO}}{M}. \tag{21}$$

Consequently,

$$\sigma^{\rm naive}_{f_{\rm ISCO}} = \left|\frac{\partial f_{\rm ISCO}}{\partial M}\right| \sigma_M = f_{\rm ISCO}\frac{\sigma_M}{M}, \tag{22}$$

where σ_M is the naive FIM prediction for the mass measurement uncertainty, $\sigma_M^2 = (\Gamma^{-1})_{MM}$.

When the condition

$$\sigma^{\rm naive}_{f_{\rm ISCO}} \ll \sigma^{\rm abrupt}_{f_{\rm ISCO}} \tag{23}$$

holds, there is little information content in the waveform cutoff, and it is generally safe to ignore the impact of the cutoff on parameter estimation. However, if this condition is violated, the information from the abrupt cutoff can significantly reduce parameter-estimation uncertainty. For example, for a noise spectrum roughly representative of initial LIGO sensitivity [35], which was used in [44], $\sigma^{\rm naive}_{f_{\rm ISCO}} \approx \sigma^{\rm abrupt}_{f_{\rm ISCO}}$ at a total mass of approximately $15M_\odot$ at $\rho = 10$ (higher SNR makes the abrupt cutoff significant at lower masses). Thus, for this noise spectrum, (23) holds for low-mass binaries such as neutron-star–neutron-star and low mass neutron-star–black-hole systems, but is violated for comparable-mass black-hole systems of $\gtrsim 10M_\odot$.

3.3. Analytic approximation of the full likelihood

We can incorporate correlations of $f_{\rm ISCO}$ with an arbitrary number of waveform parameters by a suitable combination of the FIM approximation and the linearization introduced in (11). We follow the approach of Ohme *et al.* [17] who noted that in the case of a parameter-dependent cutoff frequency, the log likelihood (5), with $d = h(\vec{\theta}_0)$, can be expressed to leading order as

$$\log L(\vec{\theta}) \approx -\frac{1}{2}\left(\sum_{i,\,j}\Gamma_{ij}\Delta\theta_i\Delta\theta_j + 4\left|\int_{f_1}^{f_2}\zeta(f)\,\mathrm{d}f\right|\right). \tag{24}$$

The first term constitutes the standard (naive) FIM approximation in the frequency range up to the cutoff frequency of the reference signal, and the second term accounts for the fact that the (ISCO) cutoff frequencies f_1 and f_2 can differ between the two waveforms.

The linear-order expansion of the second term is a generalization of (11) and reads

$$4\left|\int_{f_1}^{f_2}\zeta(f)\,\mathrm{d}f\right| \approx 4\zeta(f_{\rm ISCO})\left|\sum_i \frac{\partial f_{\rm ISCO}}{\partial\theta_i}\Delta\theta_i\right|. \tag{25}$$

We recast the last expression in terms of

$$\Delta\hat{\theta}_j \equiv 2\zeta(f_{\rm ISCO})\sum_k \left(\Gamma^{-1}\right)_{jk}\frac{\partial f_{\rm ISCO}}{\partial\theta_k}, \tag{26}$$

leading to

$$4\left|\int_{f_1}^{f_2}\zeta(f)\,\mathrm{d}f\right| \approx 2\left|\sum_{i,\,j}\Gamma_{ij}\Delta\theta_i\Delta\hat{\theta}_j\right|. \tag{27}$$

Combining (27) with (24) and using the symmetry of Γ_{ij} finally leads to

$$\log L(\vec{\theta}) \approx -\frac{1}{2}\left(\sum_{i,\,j}\Gamma_{ij}\Delta\theta_i\Delta\theta_j + 2\left|\sum_{i,\,j}\Gamma_{ij}\Delta\theta_i\Delta\hat{\theta}_j\right|\right) \tag{28}$$

$$= -\frac{1}{2}\sum_{i,\,j}\Gamma_{ij}\left(\Delta\theta_i \pm \Delta\hat{\theta}_i\right)\left(\Delta\theta_j \pm \Delta\hat{\theta}_j\right) + \mathcal{C}. \tag{29}$$

The signs in the expression above are all positive when $\sum_{i,\,j}\Gamma_{ij}\Delta\theta_i\Delta\hat{\theta}_j$ is positive, and negative otherwise. The constant $\mathcal{C} = \sum_{i,\,j}\Gamma_{ij}\Delta\hat{\theta}_i\Delta\hat{\theta}_j/2$ simply corrects the overall shift in $\log L$ introduced by completing the square.

Despite the issue of picking the correct sign for $\Delta\hat{\theta}_i$, (29) is easy to interpret. The marginalised likelihood over all but one parameter is a piecewise Gaussian function with the peak displaced by $\mp\Delta\hat{\theta}_i$, and the sign is chosen such that the peak lies on the negative/positive axis for positive/negative perturbations. A one-dimensional illustration is provided by Fig. 1.

This combination of two displaced Gaussian functions has a sharp peak at the maximum $\Delta\theta_i = 0$ and a faster fall-off around the peak than the (naive) FIM prediction. Thus, parameter-estimation studies (such as [44]) that properly take the abrupt cutoff

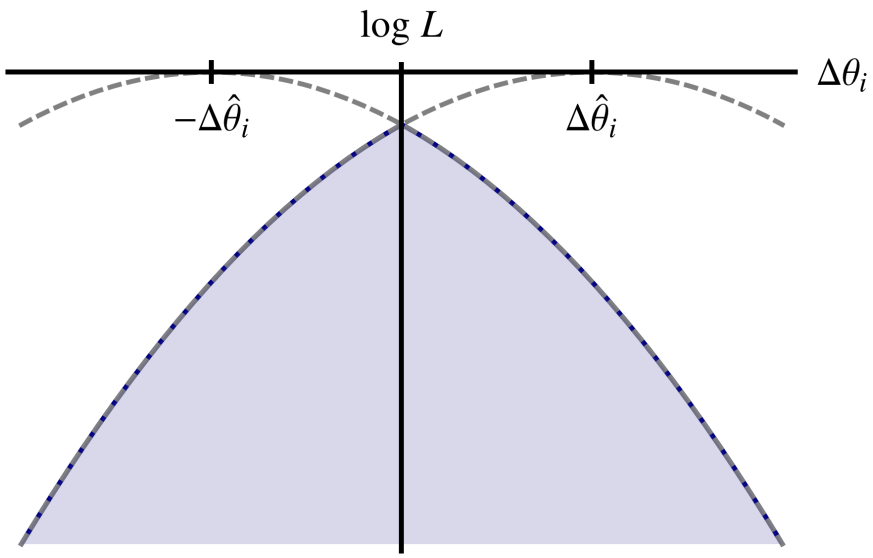

Figure 1. An illustration of the shape of $\log L$ as derived in (29), marginalised over all other parameters. An abrupt cutoff in the frequency domain manifests itself at linear order as a symmetric displacement of the Gaussian likelihood by $\Delta\hat{\theta}_i$, cf. (26). The curve bounding the shaded area constitutes the resulting log likelihood that is continuous, but not differentiable at the origin.

into account predict better parameter-estimation accuracy than is achievable when such an artificial cutoff does not exist. Of course, if the displacement $\Delta\hat{\theta}_i$ is small compared to the typical parameter variations defined by the problem in question, then the overall effect of an abrupt cutoff is small. In contrast, larger values of $|\Delta\hat{\theta}_i|$ increase the effect of an abrupt parameter-dependent cutoff.

In our case, the natural parameter variation we should compare to is given by the standard deviation σ_i of the (naive) FIM prediction. The change in the likelihood function is significant only when the deviation $\Delta\hat{\theta}_i$ is significant relative to this variation. Hence, we can neglect the effect of a parameter-dependent cutoff frequency if

$$|\Delta\hat{\theta}_i| \ll \sigma_i, \tag{30}$$

which is a generalization of the toy case we discussed in the previous subsection. For the simple case of a single parameter M, the condition (23) becomes

$$|\Delta\hat{M}| \ll \sqrt{2}\sigma_M, \tag{31}$$

consistent with (30).

One can draw several conclusions from these considerations and the explicit form of $\Delta\hat{\theta}_i$ given in (26). First, $\Delta\hat{\theta}_i$ is proportional to $\zeta(f_{\rm ISCO})$. This confirms in full generality that an abrupt cutoff can be safely ignored if the waveform amplitude at this cutoff frequency is buried deep in the instrument noise. This is the case for typical binary neutron-star systems observed with initial- and advanced-generation GW detectors at reasonable SNR.‖

‖ The left-hand side of (31) is independent of distance with all other parameters fixed, while the right-hand side scales inversely with SNR or linearly with distance, so the abrupt cutoff could still be

Furthermore, although the frequently-employed ISCO cutoff frequency only depends on the total mass M for binaries with non-spinning components, all parameters that are *correlated* with M are affected by the sharp cutoff as well. This becomes apparent in (26), where the gradient of the cutoff frequency is contracted with the inverse FIM (which becomes the correlation matrix in the high-SNR limit). Conversely, parameters that are not significantly correlated with the total mass (e.g., the sky location in a network of identical detectors) are not affected.

Last, both (29) and Fig. 1 demonstrate that $\log L$ is *not* differentiable at the origin, a fact that immediately puts the practicability and possible interpretation of a FIM study into question. We discuss this in more detail in the next subsection.

3.4. Including an abrupt waveform cutoff in the FIM

In view of the above, it is perhaps not surprising that a full FIM, which takes all previously discussed effects into account, is not well defined (at any SNR) when an abrupt waveform cutoff is present. The FIM, by construction, predicts parameter uncertainties that scale inversely with ρ, whereas information from an abrupt cutoff makes it possible to measure parameters with an accuracy that scales inversely with ρ^2. Regardless of the SNR, it is impossible to accurately capture the character of the sharp peak in the log likelihood with a quadratic function. The gradient of the log likelihood is undefined at the true parameters when the log likelihood has a sharp peak that renders its derivatives discontinuous.

When the waveform has an abrupt cutoff, as in (2), its derivative with respect to parameters includes an additional term proportional to the derivative of the Heaviside function, namely a delta function. The full derivative $\tilde{h}_{,i}$ is

$$\tilde{h}_{,i} = \tilde{h}^0_{,i} - \tilde{h}^0 \delta(f_{\rm ISCO} - f) \frac{\partial f_{\rm ISCO}}{\partial \theta_i}, \tag{32}$$

where

$$\tilde{h}^0_{,i} = \left[\frac{\partial A(f)}{\partial \theta_i} + iA \frac{\partial \Psi(f)}{\partial \theta_i} \right] \exp\left[i\Psi(f) \right] H(f_{\rm ISCO} - f) \tag{33}$$

is the only part of the derivative included in standard calculations.

We can substitute (32) into (8) to calculate the full FIM, which we denote $\check{\Gamma}_{ij}$. The full FIM comprises the terms we have previously considered, the naive, inspiral-only $\Gamma_{ij} \equiv \left\langle \tilde{h}^0_{,i} \middle| \tilde{h}^0_{,j} \right\rangle$, and additional terms that occur whenever the cutoff $f_{\rm ISCO}$ depends on the parameters θ_i or θ_j. When the derivatives of $f_{\rm ISCO}$ with respect to both θ_i and θ_j are non-zero, $\check{\Gamma}_{ij}$ includes a term that is proportional to the integral of a squared delta function, which is formally undefined, but can be considered infinite for this application.

The naive FIM Γ_{ij}, which is commonly used in calculations, is incomplete for a waveform with abrupt cutoffs. This incompleteness can result in apparent violations of the Cramér–Rao bound. Rodriguez *et al.* [44] found that the naive FIM can overestimate

significant for nearby low-mass sources. However, even for a binary with two $3M_\odot$ components, this would only happen at $\rho \gtrsim 100$.

uncertainties in mass parameters by a factor of 5–10 for binary black holes with total mass approaching $20M_\odot$, i.e., in the regime where $\sigma^{\rm naive}_{f_{\rm ISCO}} \gg \sigma^{\rm abrupt}_{f_{\rm ISCO}}$ (or, equivalently, $\Delta\hat{\theta}_i \gg \sigma_i$ for parameter of interest θ_i) and the information contents of the cutoff is significant. On the other hand, the naive FIM yields uncertainty estimates compatible with a full Bayesian analysis that incorporates information from the cutoff at binary neutron-star masses, where $\sigma^{\rm naive}_{f_{\rm ISCO}} \ll \sigma^{\rm abrupt}_{f_{\rm ISCO}}$ ($\Delta\hat{\theta}_i \ll \sigma_i$) and the information content of the abrupt waveform termination is minimal (see Fig. 1 of [44]).

Meanwhile, the full FIM is ill-defined. Therefore, the FIM cannot be used when the waveforms have abrupt cutoffs. It is possible to regularize the FIM by replacing the step function with a more gradual taper, and progressively making the taper more abrupt. As an example of this, we consider measurements of the chirp mass

$$\mathcal{M} = \frac{(m_1 m_2)^{3/5}}{M^{1/5}}\,; \tag{34}$$

we find that the inverse FIM element $(\check{\Gamma}^{-1})_{\mathcal{M}\mathcal{M}}$ can be reduced by many orders of magnitude relative to the usual (and incomplete) calculation that only considers $(\Gamma^{-1})_{\mathcal{M}\mathcal{M}}$. For instance, for a binary neutron-star system with $m_{1,\,2} = 1.4M_\odot$ and the waveform model and noise model of [44], we find that the full $(\check{\Gamma}^{-1})_{\mathcal{M}\mathcal{M}}$ is reduced by a factor of $\sim 10^9$ relative to the naive calculation. A complete FIM with a regularized abrupt cutoff does act as a Cramér–Rao bound, resolving the apparent violation noted in [44], but it is a useless extreme lower bound on the mass parameters, underestimating the chirp mass uncertainty by a factor of $\sim 10^4$.

In the calculation above, we considered continuous integrals; in practice, data analysis relies on discretized data and templates. There are potentially two ways to discretize a waveform with an abrupt cutoff. In order to preserve the correct total waveform power, the waveform amplitude in the last non-zero frequency bin can be weighted to account for the value of the cutoff (ISCO) frequency. This procedure yields the same results as in the continuous limit discussed above. Alternatively, if no weighting is used, the waveform is insensitive to changes of the cutoff frequency so long as the cutoff remains between frequency samples, and the likelihood is quadratic; a sample is abruptly added or removed from the waveform only when the cutoff frequency moves to a neighbouring bin, causing a discontinuous step in the likelihood. If the frequency-domain sampling step is larger than $\sigma^{\rm abrupt}_{f_{\rm ISCO}}$, the naive FIM calculation should apply; otherwise, the sharply peaked likelihood of Fig. 1 is replaced by a terraced shape, which yields the same limiting behaviour as the sampling step gets smaller.

4. Abruptly terminating templates and complete signals

We detailed in the previous section how an abrupt signal termination in the frequency domain affects the recovery of source parameters. The underlying assumption that both signal and template contain such a cutoff yielded an artificial increase in information. There are, however, only a few cases where we would expect a real signal to terminate abruptly, e.g., coalescing extreme-mass-ratio inspirals, where the plunge is rapid, and the

merger and ringdown have almost no power relative to the inspiral [48], or inspiralling stars that are tidally disrupted by their black-hole companion before merger; and even in those cases the falloff could be abrupt in the time domain, but not necessarily in the frequency domain. In most other cases, we do not expect real GW signals to exhibit such an abrupt cutoff at all. Thus, the results derived in Sec. 3 do not apply immediately to typical GW searches.

Ideally, one should use waveform templates that actually model the entire inspiral–merger–ringdown structure of the expected signals whenever a sharp frequency cutoff has a considerable effect on the measurement as discussed around (30). Nevertheless, there are cases where this is either not practical or not possible, and performing GW measurements with accurate inspiral waveforms, neglecting merger and ringdown, can have considerable computational advantages (e.g., [43, 39]). This section provides some discussion of how our previously derived results change if abruptly terminating templates but complete signals are considered. This allows us to determine an approximate region of mass space for which the use of abruptly terminating waveforms for tasks such as template placement, gravitational-wave searches and parameter estimation is reasonable.

To do so, we consider the best-case scenario, where the real signal and the corresponding waveform template agree perfectly up to the template cutoff frequency $f_{\rm ISCO}(\theta)$. We then find

$$\log L(\vec{\theta}) = -\frac{1}{2}\left(\langle \Delta h|\Delta h\rangle\Big|_0^{f_{\rm ISCO}} + 4\int_{f_{\rm ISCO}}^{\infty} \zeta(f)\,\mathrm{d}f\right), \tag{35}$$

which is similar to (24), although in this case the template waveform is guaranteed to end at a lower frequency than the signal. An important difference, however, is that unlike the likelihood in (24) which contains an absolute value, this likelihood is everywhere smooth and differentiable (see Fig. 2 and discussion below). Therefore, we expect to be able to carry out a Taylor expansion around the best-fit parameters and describe the covariance with an appropriate FIM calculation.

The inner product $\langle \Delta h|\Delta h\rangle$ is restricted to the frequency range where both signal and template are nonvanishing, $f \in [0, f_{\rm ISCO}]$. We can approximate it with the naive, inspiral-only FIM that is well defined in this regime. The second contribution has a nontrivial dependence on the actual shape of the merger and ringdown amplitude, but we approximate it for small parameter variations to first order as

$$\begin{aligned} 4\int_{f_{\rm ISCO}}^{\infty} \zeta(f)\mathrm{d}f &\approx \rho^2_{\rm MR} - 4\zeta(f_{\rm ISCO})\Delta f_{\rm ISCO} \\ &\approx \rho^2_{\rm MR} - 4\zeta(f_{\rm ISCO})\sum_i \frac{\partial f_{\rm ISCO}}{\partial\theta_i}\Delta\theta_i, \end{aligned} \tag{36}$$

where $\Delta f_{\rm ISCO} \equiv f_{\rm ISCO}(\vec{\theta}) - f_{\rm ISCO}(\vec{\theta}_0)$. The power contained in the merger and ringdown $\rho^2_{\rm MR}$ quantifies the loss in efficiency when we search with an incomplete (but otherwise perfectly matching) model. It is constant in this expansion and we neglect it as it is a pure scaling factor that does not affect the shape of L.

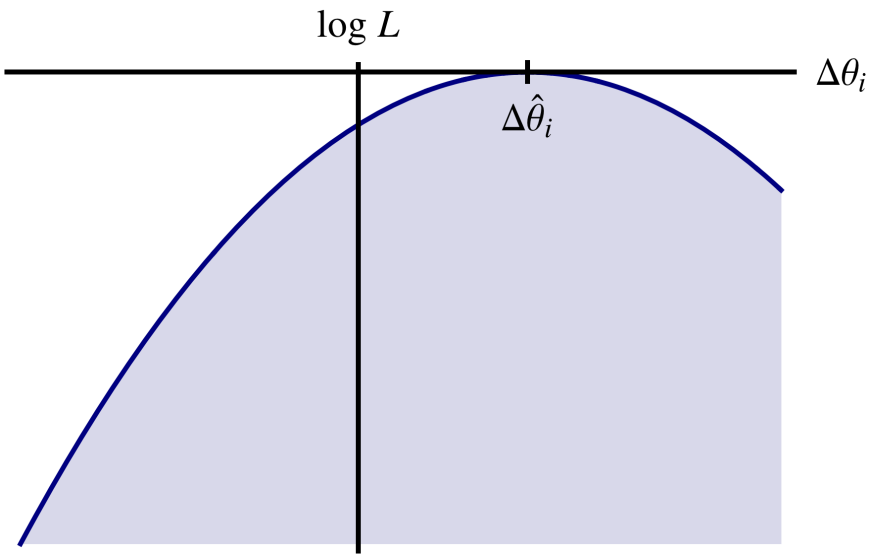

Figure 2. A one-dimensional illustration of the shape of $\log L$ as derived in (37). Parameter estimation on a complete signal with an abruptly terminated template family leads to a systematic bias $\Delta\hat{\theta}_i$, cf. (26).

Then, by comparison with (25)–(29) we find that

$$\log L(\vec{\theta}) \sim -\frac{1}{2}\sum_{i,j}\Gamma_{ij}\left(\Delta\theta_i - \Delta\hat{\theta}_i\right)\left(\Delta\theta_j - \Delta\hat{\theta}_j\right), \tag{37}$$

where we have dropped all additional contributions that are parameter-independent (again, they do not affect the shape of L) and $\Delta\hat{\theta}_i$ is given by (26).

The obvious difference between (29) and (37) is that in the case of a full signal, the displacement vector $\Delta\hat{\theta}_i$ remains constant independent of the sign of the parameter perturbations. The reason is that previously, any deviation from the target cutoff frequency resulted in an increase of the waveform difference. Now, however, an increase in the template cutoff frequency can improve the match with the target signal because a wider frequency range is covered by the template with different parameters.

Fig. 2 illustrates the behaviour of $\log L$ as derived in (37). The width of the likelihood or, more generally, the parameter covariance, is the same as predicted by a naive FIM that represents a smoothly terminating inspiral-only calculation. We are generally justified in ignoring second-order terms to the expansion (36), which formally constitute a correction to the naive inspiral FIM, as they are governed by small additions to the signal power from the parameter-dependent cutoff, but we discuss the validity of this below. The main effect is a displacement of the peak of $\log L$ by $\Delta\hat{\theta}_i$, which can be identified as a systematic bias caused by the disagreement between the full signal and the template waveform models. Since we have assumed that signal and template models match perfectly up to $f_{\rm ISCO}$, it is only the fact that the signal extends to higher frequencies than the cutoff template which introduces the bias

$$\mathrm{E}[\Delta\theta_i] = \Delta\hat{\theta}_i, \tag{38}$$

where $\Delta\hat{\theta}_i$ are given by (26).

Let us consider the case where the template terminates at $f_{\rm ISCO}$, which is a function of only the total mass as given by (19). Taking $\sigma_M^2 = (\Gamma^{-1})_{MM}$ we find

$$\Delta\hat{M} = -2 f_{\rm ISCO}\, \zeta(f_{\rm ISCO}) \frac{\sigma_M^2}{M}. \tag{39}$$

where, as before ζ is the noise-weighted signal power as given in (12). As expected, a search with abruptly terminating templates tends to underestimate the total mass to cover a larger frequency range.

If we analyze a full signal with abruptly cutoff templates that faithfully reproduce the inspiral-only portion of the signal, we expect to find that both fractional statistical uncertainties and systematic biases on the mass parameter increase as the binary mass increases. The relative statistical uncertainty increases as fewer inspiral cycles are in the detector band for high-mass signals. The increase in the systematic bias is even more rapid because of the quadratic dependence on uncertainty in (39) and because the noise-weighted power $\zeta(f_{\rm ISCO})$ increases as the cutoff frequency is lowered towards the most sensitive frequency region of the detector.

To illustrate the order of magnitude of this effect, we calculate inspiral-only FIMs for binaries consisting of a $m_2 = 1.35 M_\odot$ neutron star and a black hole with a mass m_1 between $5M_\odot$ and $20M_\odot$. All target systems have non-spinning components, but our FIM calculation takes variations of the black-hole spin into account, although we constrain spins to be aligned with the orbital angular momentum so that the system does not undergo precession. We employ a frequency-domain post-Newtonian waveform model of the form (1), and details of our implementation are given in [17]. Although we are now considering the search for complete signals, our first-order expansion framework does not require us to use any specific merger–ringdown model. We assume a network SNR of 10 (accumulated up to $f_{\rm ISCO}$) for identical detectors characterized by the Advanced LIGO noise curve in the zero-detuned high-power configuration [49], with a lower frequency cutoff at 10 Hz.

In Fig. 3 we plot the statistical uncertainty in measuring the chirp mass $\sigma_{\mathcal{M}}$ and the bias caused by an abruptly ending template $\Delta\hat{\mathcal{M}}$. As expected, both the statistical uncertainty and systematic bias increase with increasing mass. However, the systematic bias increases more rapidly and becomes the dominant contribution at black-hole masses $m_1 \gtrsim 10M_\odot$. Buonanno *et al.* [37] estimated the mass at which the merger and ringdown contribute a significant fraction to the SNR (specifically, where the effectualness drops to 0.97) at $12M_\odot$ for the same detector configuration. Our calculation, which is concerned with parameter bias for threshold signals, provides a similar cutoff. For louder signals, the statistical uncertainties are reduced, such that merger and ringdown can play an important part at lower masses.

Another related conclusion applies to template-placement algorithms that are based on the FIM normalized by the squared SNR [50, 51, 52, 53]. Commonly, such template banks are constructed by requiring that signals and the nearest template have a match of at least 0.97. Our results show that the naive, inspiral-only FIM prediction is

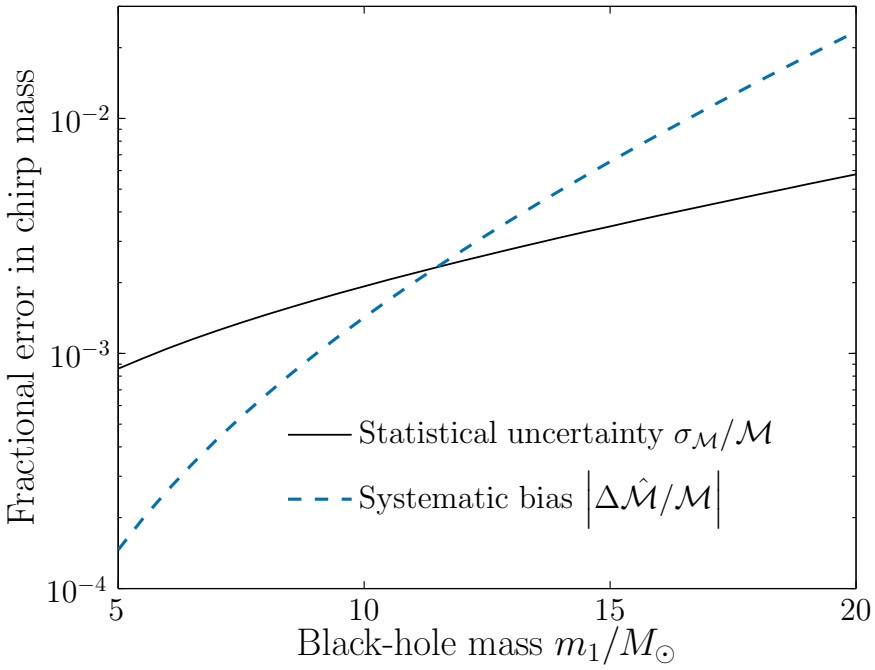

Figure 3. Relative statistical uncertainty $\sigma_{\mathcal{M}}/\mathcal{M}$ (solid line) and systematic bias $\Delta\hat{\mathcal{M}}/\mathcal{M}$ (dashed line) caused by using abruptly terminating templates, here shown for non-spinning binaries with a $m_2 = 1.35M_\odot$ neutron star and a black hole with the indicated mass m_1 at $\rho = 10$. The underlying FIM allows variations of both masses, the black-hole spin (aligned with the orbital angular momentum), as well as reference time and phase. The assumed detector is Advanced LIGO (zero-detuned high-power configuration) with a lower cutoff at 10 Hz [49].

still applicable for abruptly terminating templates, in case they are used to search for complete signals. There is an additional systematic bias that, in principle, does not harm the detection efficiency, but should be taken into account when identifying the parameter range of the search or quoting the parameters of the template with the highest data correlation.

This systematic bias only becomes important when it is comparable or larger than the template discretization, i.e., when $\Delta\hat{\theta}_i$ is outside the 0.97 match region of the respective template. For constant SNR (which is a sufficiently good approximation of optimized template SNRs) we can use

$$\frac{1}{\rho^2}\left\langle h(\vec{\theta}_0)\middle|h(\vec{\theta})\right\rangle \approx 1 - \frac{1}{2\rho^2}\sum_{i,\,j}\Gamma_{ij}\Delta\theta_i\Delta\theta_j \tag{40}$$

(see [17]) to relate a 0.97 match on the left-hand side of (40) with a statistical uncertainty predicted by the FIM. We find that the marginalized one-dimensional standard deviation σ_i is equivalent to matches of 0.97 if $\rho \approx 4$. Thus, if considering neutron-star–black-hole searches, one would have to increase the statistical uncertainty in Fig. 3 accordingly to find that the systematic bias dominates in template banks for black-hole masses $m_1 \gtrsim 17M_\odot$.

The above analysis was performed to leading order, and the example given for a

specific binary source and detector configuration; thus, while it gives a reasonable rule of thumb as to when the systematic effect of neglecting merger and ringdown may become important, it should not be naively applied in all situations. In particular, any time the systematic error becomes comparable to the statistical uncertainty, expanding linearly around the true parameters is no longer guaranteed to produce meaningful results. Quadratic terms like $\mathrm{d}\zeta/\mathrm{d}f_{\mathrm{ISCO}}\,(\Delta f_{\mathrm{ISCO}})^2$ need to be included, though for sufficiently large biases, the expansion around the true parameters may not converge.

In summary, this calculation can explain systematic biases and predict their general trend (i.e., small masses are favoured), but the actual value sensitively depends on more waveform features than those taken into account here. Moreover, while abrupt template termination does not introduce unwarranted measurement accuracy in the case when a full signal is considered and systematic biases are small, using incomplete templates without merger and ringdown contributions leads to an overly pessimistic prediction of measurement uncertainty.

5. Conclusion

We have studied the influence of an abrupt waveform cutoff on parameter estimation. Abrupt cutoffs are often used in GW astronomy because of the uncertainty in the merger and ringdown components of the waveform, or for ease of computation. However, terminating the waveform can have undesired consequences if this occurs in the band of the detectors, that is if there is significant noise-weighted power at the cutoff frequency. It is therefore desirable to use complete inspiral–merger–ringdown waveforms. If these are not used, there are a number of effects to be aware of.

We have shown that there is potentially a significant amount of information encoded in the (in-band) abrupt termination of waveforms. They may appear to provide more information than is available in practice. Therefore, studies using abruptly terminated signals and templates may overstate the accuracy with which parameters can be recovered. In this paper, we evaluated the information contained in such a cutoff, determined when it was significant, and described how it could be approximately incorporated into an analytic calculation. Although this study was based on frequency-domain waveforms, we expect the abrupt termination of time-domain waveforms to yield analogous additional information in the cutoff; however, in practice, abruptly terminating time-domain waveforms are often tapered to avoid artifacts when transforming into the frequency domain, which ameliorates this effect.

The naive FIM calculation is blind to the information encoded in the abrupt cutoffs.¶ This can create a difference between various approaches for measuring

¶ All our analysis has been performed within a linearized framework. Therefore, many of our formulae are only directly applicable when considering small changes in parameters, just as the inverse FIM can only be used to estimate the covariance in the linear-signal approximation. Our colleagues [54] further developed the present work by demonstrating the impact of abruptly terminating templates within the effective Fisher Information Matrix formalism [18].

parameter-estimation accuracy when the same models are used, and can cause an apparent violation of the Cramér–Rao bound. It also means that the naive, inspiral-only FIM can give incorrect, overly pessimistic predictions if the physical model really does call for an abrupt cutoff.

While full parameter estimation with abruptly terminated waveforms incorporates unphysical information from the waveform termination, which can artificially improve parameter estimation accuracy, and the naive FIM calculation avoids this problem, both ignore the information contained beyond the cutoff frequency, in the merger and ringdown phases of the waveform. Thus, there is a potential trade-off between the artificial gain of information from the sharp cutoff and the real loss of information from neglecting the merger and ringdown phases.

The above results were obtained assuming that both the true signal and waveform template include a cutoff. Using abruptly terminated waveform templates to analyse a complete, non-terminating signal leads to a bias in the estimated parameters. This is not surprising, since the templates do not match their target signals. We have shown how to estimate the size of the bias, provided that it is sufficiently small that the linearized framework remains valid.

In addition, we have shown that at lowest order the FIM prediction of parameter covariances remains unaffected by the template cutoff if the signal to be searched for actually extends to higher frequencies. This proves, in hindsight, that previous FIM results in the literature are meaningful, even for heavier systems containing black holes, if interpreted in the way outlined here. However, if the merger and ringdown power is significant, parameters could be extracted more accurately with full inspiral–merger–ringdown analyses than predicted by the naive, inspiral-only FIM, so these studies may be overly pessimistic for massive systems.

An interesting application of this final result is to algorithms that build template banks for GW searches based on inspiral-only FIM predictions. Our analysis indicates that such banks still cover the waveform manifold as desired if the underlying abruptly terminating templates are used to search for complete signals. However, the loss in SNR, as well as the above-mentioned bias, generally remain unaccounted for.

It is important to take care of the unintended consequences of using unphysical models with sharp cutoffs. The best solution for obtaining accurate estimates for parameter uncertainties lies in the use of waveforms that faithfully capture the merger and ringdown phases, cf. [37, 27, 55, 39].

Acknowledgments

The authors are grateful to colleagues from the Birmingham GW astrophysics group, the Cardiff gravitational physics group and the LIGO–Virgo Science Collaborations. This work was supported by the Science and Technology Facilities Council and a Leverhulme Trust research project grant.

References

[1] B. Abbott et al. LIGO: The Laser Interferometer Gravitational-Wave Observatory. *Rept. Prog. Phys.*, 72:076901, 2009, 0711.3041.

[2] T. Accadia, F. Acernese, M. Alshourbagy, P. Amico, F. Antonucci, S. Aoudia, N. Arnaud, C. Arnault, K. G. Arun, P. Astone, et al. Virgo: a laser interferometer to detect gravitational waves. *J. Instrum.*, 7:3012, March 2012.

[3] G. M. Harry et al. Advanced LIGO: the next generation of gravitational wave detectors. *Class. Quant. Grav.*, 27(8):084006, April 2010.

[4] F. Acernese et al. Advanced virgo baseline design. Virgo Technical Report VIR-0027A-09, 2009.

[5] J. Aasi and et al. Prospects for Localization of Gravitational Wave Transients by the Advanced LIGO and Advanced Virgo Observatories. *ArXiv e-prints*, April 2013, 1304.0670.

[6] J. Abadie et al. Predictions for the Rates of Compact Binary Coalescences Observable by Ground-based Gravitational-wave Detectors. *Class. Quant. Grav*, 27(17):173001, September 2010, 1003.2480.

[7] M. Vallisneri. Use and abuse of the Fisher information matrix in the assessment of gravitational-wave parameter-estimation prospects. *Phys. Rev. D*, 77(4):042001, February 2008, gr-qc/0703086.

[8] L. S. Finn. Detection, measurement, and gravitational radiation. *Phys. Rev. D*, 46:5236–5249, December 1992, gr-qc/9209010.

[9] C. Cutler and É. E. Flanagan. Gravitational waves from merging compact binaries: How accurately can one extract the binary's parameters from the inspiral waveform? *Phys. Rev. D*, 49:2658–2697, March 1994, gr-qc/9402014.

[10] E. Poisson and C. M. Will. Gravitational waves from inspiraling compact binaries: Parameter estimation using second-post-Newtonian waveforms. *Phys. Rev. D*, 52:848–855, July 1995, gr-qc/9502040.

[11] C. L. Rodriguez, I. Mandel, and J. R. Gair. Verifying the no-hair property of massive compact objects with intermediate-mass-ratio inspirals in advanced gravitational-wave detectors. *Phys. Rev. D*, 85(6):062002, March 2012, 1112.1404.

[12] A. Pai and K. G. Arun. Singular value decomposition in parametrized tests of post-Newtonian theory. *Class. Quant. Grav.*, 30(2):025011, January 2013, 1207.1943.

[13] S. Fairhurst. Triangulation of gravitational wave sources with a network of detectors. *New J. Phys.*, 11(12):123006, December 2009, 0908.2356.

[14] S. Fairhurst. Source localization with an advanced gravitational wave detector network. *Class. Quant. Grav.*, 28(10):105021, May 2011, 1010.6192.

[15] K. Grover, S. Fairhurst, B. F. Farr, I. Mandel, C. Rodriguez, T. Sidery, and A. Vecchio. Comparison of gravitational wave detector network sky localization approximations. *Phys. Rev. D*, 89(4):042004, February 2014, 1310.7454.

[16] M. Hannam, D. A. Brown, S. Fairhurst, C. L. Fryer, and I. W. Harry. When can Gravitational-wave Observations Distinguish between Black Holes and Neutron Stars? *Astrophys. J. Lett.*, 766:L14, March 2013, 1301.5616.

[17] F. Ohme, A. B. Nielsen, D. Keppel, and A. Lundgren. Statistical and systematic errors for gravitational-wave inspiral signals: A principal component analysis. *Phys. Rev. D*, 88(4):042002, August 2013, 1304.7017.

[18] H.-S. Cho, E. Ochsner, R. O'Shaughnessy, C. Kim, and C.-H. Lee. Gravitational waves from black hole-neutron star binaries: Effective Fisher matrices and parameter estimation using higher harmonics. *Phys. Rev. D*, 87(2):024004, January 2013, 1209.4494.

[19] E. T. Jaynes. *Probability Theory: The Logic of Science*. Cambridge University Press, April 2003.

[20] M. van der Sluys, V. Raymond, I. Mandel, C. Röver, N. Christensen, V. Kalogera, R. Meyer, and A. Vecchio. Parameter estimation of spinning binary inspirals using Markov chain Monte Carlo. *Class. Quant. Grav.*, 25(18):184011, September 2008, 0805.1689.

[21] J. Veitch and A. Vecchio. Bayesian coherent analysis of in-spiral gravitational wave signals with a detector network. *Phys. Rev. D*, 81(6):062003, March 2010, 0911.3820.

[22] V. Raymond, M. V. van der Sluys, I. Mandel, V. Kalogera, C. Röver, and N. Christensen. The effects of LIGO detector noise on a 15-dimensional Markov-chain Monte Carlo analysis of gravitational-wave signals. *Class. Quant. Grav.*, 27(11):114009, June 2010, 0912.3746.

[23] J. Veitch, I. Mandel, B. Aylott, B. Farr, V. Raymond, C. Rodriguez, M. van der Sluys, V. Kalogera, and A. Vecchio. Estimating parameters of coalescing compact binaries with proposed advanced detector networks. *Phys. Rev. D*, 85:104045, 2012, 1201.1195.

[24] C. L. Rodriguez, B. Farr, V. Raymond, W. M. Farr, T. B. Littenberg, D. Fazi, and V. Kalogera. Basic Parameter Estimation of Binary Neutron Star Systems by the Advanced LIGO/Virgo Network. *Astrophys. J.*, 784:119, April 2014, 1309.3273.

[25] U. Sperhake, E. Berti, and V. Cardoso. Numerical simulations of black-hole binaries and gravitational wave emission. *ArXiv e-prints*, July 2011, 1107.2819.

[26] H. P. Pfeiffer. Numerical simulations of compact object binaries. *Class. Quant. Grav.*, 29(12):124004, June 2012, 1203.5166.

[27] F. Ohme. Analytical meets numerical relativity: status of complete gravitational waveform models for binary black holes. *Class. Quant. Grav.*, 29(12):124002, June 2012, 1111.3737.

[28] L. Santamaría, F. Ohme, P. Ajith, B. Brügmann, N. Dorband, M. Hannam, S. Husa, P. Mösta, D. Pollney, C. Reisswig, E. L. Robinson, J. Seiler, and B. Krishnan. Matching post-Newtonian and numerical relativity waveforms: Systematic errors and a new phenomenological model for nonprecessing black hole binaries. *Phys. Rev. D*, 82(6):064016, September 2010, 1005.3306.

[29] P. Ajith. Addressing the spin question in gravitational-wave searches: Waveform templates for inspiralling compact binaries with nonprecessing spins. *Phys. Rev. D*, 84(8):084037, October 2011, 1107.1267.

[30] Y. Pan, A. Buonanno, M. Boyle, L. T. Buchman, L. E. Kidder, H. P. Pfeiffer, and M. A. Scheel. Inspiral-merger-ringdown multipolar waveforms of nonspinning black-hole binaries using the effective-one-body formalism. *Phys. Rev. D*, 84(12):124052, December 2011, 1106.1021.

[31] A. Taracchini, Y. Pan, A. Buonanno, E. Barausse, M. Boyle, T. Chu, G. Lovelace, H. P. Pfeiffer, and M. A. Scheel. Prototype effective-one-body model for nonprecessing spinning inspiral-merger-ringdown waveforms. *Phys. Rev. D*, 86(2):024011, July 2012, 1202.0790.

[32] A. Taracchini, A. Buonanno, Y. Pan, T. Hinderer, M. Boyle, D. A. Hemberger, L. E. Kidder, G. Lovelace, A. H. Mroué, H. P. Pfeiffer, M. A. Scheel, B. Szilágyi, N. W. Taylor, and A. Zenginoglu. Effective-one-body model for black-hole binaries with generic mass ratios and spins. *Phys. Rev. D*, 89(6):061502, March 2014, 1311.2544.

[33] T. Damour, A. Nagar, and S. Bernuzzi. Improved effective-one-body description of coalescing nonspinning black-hole binaries and its numerical-relativity completion. *Phys. Rev. D*, 87(8):084035, April 2013, 1212.4357.

[34] L. Blanchet. Gravitational Radiation from Post-Newtonian Sources and Inspiralling Compact Binaries. *Living Reviews in Relativity*, 17:2, February 2014, 1310.1528.

[35] T. Damour, B. R. Iyer, and B. S. Sathyaprakash. Comparison of search templates for gravitational waves from binary inspiral. *Phys. Rev. D*, 63(4):044023, February 2001, gr-qc/0010009.

[36] T. Damour, B. R. Iyer, and B. S. Sathyaprakash. Comparison of search templates for gravitational waves from binary inspiral: 3.5PN update. *Phys. Rev. D*, 66(2):027502, July 2002, gr-qc/0207021.

[37] A. Buonanno, B. R. Iyer, E. Ochsner, Y. Pan, and B. S. Sathyaprakash. Comparison of post-Newtonian templates for compact binary inspiral signals in gravitational-wave detectors. *Phys. Rev. D*, 80(8):084043, October 2009, 0907.0700.

[38] S. Vitale and M. Zanolin. Parameter estimation from gravitational waves generated by nonspinning binary black holes with laser interferometers: Beyond the Fisher information. *Phys. Rev. D*, 82(12):124065, December 2010, 1004.4537.

[39] J. Aasi et al. Parameter estimation for compact binary coalescence signals with the first generation

gravitational-wave detector network. *Phys. Rev. D*, 88(6):062001, September 2013, 1304.1775.

[40] J. Aasi et al. The NINJA-2 project: Detecting and characterizing gravitational waveforms modelled using numerical binary black hole simulations. *ArXiv e-prints*, January 2014, 1401.0939.

[41] J. Abadie and et al. Search for gravitational waves from low mass compact binary coalescence in LIGO's sixth science run and Virgo's science runs 2 and 3. *Phys. Rev. D*, 85(8):082002, April 2012, 1111.7314.

[42] B. Allen, W. G. Anderson, P. R. Brady, D. A. Brown, and J. D. E. Creighton. FINDCHIRP: An algorithm for detection of gravitational waves from inspiraling compact binaries. *Phys. Rev. D*, 85(12):122006, June 2012, gr-qc/0509116.

[43] S. Babak, R. Biswas, P. R. Brady, D. A. Brown, K. Cannon, C. D. Capano, J. H. Clayton, T. Cokelaer, J. D. E. Creighton, T. Dent, A. Dietz, S. Fairhurst, N. Fotopoulos, G. González, C. Hanna, I. W. Harry, G. Jones, D. Keppel, D. J. A. McKechan, L. Pekowsky, S. Privitera, C. Robinson, A. C. Rodriguez, B. S. Sathyaprakash, A. S. Sengupta, M. Vallisneri, R. Vaulin, and A. J. Weinstein. Searching for gravitational waves from binary coalescence. *Phys. Rev. D*, 87(2):024033, January 2013, 1208.3491.

[44] C. L. Rodriguez, B. Farr, W. M. Farr, and I. Mandel. Inadequacies of the Fisher information matrix in gravitational-wave parameter estimation. *Phys. Rev. D*, 88(8):084013, October 2013, 1308.1397.

[45] C. P. L. Berry and J. R. Gair. Observing the Galaxy's massive black hole with gravitational wave bursts. *Mon. Not. R. Astron. Soc.*, 429(1):589–612, February 2013, 1210.2778.

[46] T. Cokelaer. Parameter estimation of inspiralling compact binaries in ground-based detectors: comparison between Monte Carlo simulations and the Fisher information matrix. *Class. Quant. Grav.*, 25(18):184007, September 2008.

[47] D. Chakrabarty, E. H. Morgan, M. P. Muno, D. K. Galloway, R. Wijnands, M. Van Der Klis, and C. B. Markwardt. Nuclear-powered millisecond pulsars and the maximum spin frequency of neutron stars. *Nature*, 424(6944):42–44, July 2003, astro-ph/0307029.

[48] P. Amaro-Seoane, J. R. Gair, M. Freitag, M. C. Miller, I. Mandel, C. J. Cutler, and S. Babak. Intermediate and extreme mass-ratio inspirals – astrophysics, science applications and detection using LISA. *Class. Quant. Grav.*, 24:113, September 2007.

[49] Advanced LIGO anticipated sensitivity curves. https://dcc.ligo.org/cgi-bin/DocDB/ShowDocument?docid=2974.

[50] B. J. Owen. Search templates for gravitational waves from inspiraling binaries: Choice of template spacing. *Phys. Rev. D*, 53:6749–6761, June 1996, gr-qc/9511032.

[51] D. Keppel, A. P. Lundgren, B. J. Owen, and H. Zhu. Parameter space metric for 3.5 post-Newtonian gravitational waves from compact binary inspirals. *Phys. Rev. D*, 88(6):063002, September 2013, 1305.5381.

[52] D. A. Brown, I. Harry, A. Lundgren, and A. H. Nitz. Detecting binary neutron star systems with spin in advanced gravitational-wave detectors. *Phys. Rev. D*, 86(8):084017, October 2012, 1207.6406.

[53] I. W. Harry, A. H. Nitz, D. A. Brown, A. P. Lundgren, E. Ochsner, and D. Keppel. Investigating the effect of precession on searches for neutron-star-black-hole binaries with Advanced LIGO. *Phys. Rev. D*, 89(2):024010, January 2014, 1307.3562.

[54] H.-S. Cho and C.-H. Lee. Application of the effective Fisher matrix to the frequency domain inspiral waveforms. *ArXiv e-prints*, March 2014, 1403.4681.

[55] L. Sampson, N. Cornish, and N. Yunes. Mismodeling in gravitational-wave astronomy: The trouble with templates. *Phys. Rev. D*, 89(6):064037, March 2014, 1311.4898.